European Journal of Medicinal Chemistry 47 (2012) 473–478

Contents lists available at SciVerse ScienceDirect

European Journal of Medicinal Chemistry

journal homepage: http://www.elsevier.com/locate/ejmech

Original article

Synthesis, molecular modeling and biological evaluation of 2-(benzylthio)-5-aryloxadiazole derivatives as anti-tumor agents

Kai Liu, Xiang Lu, Hong-Jia Zhang, Juan Sun, Hai-Liang Zhu*

State Key Laboratory of Pharmaceutical Biotechnology, Nanjing University, Nanjing 210093, People's Republic of China

ARTICLE INFO

Article history:
Received 8 July 2011
Received in revised form
9 November 2011
Accepted 9 November 2011
Available online 18 November 2011

Keywords:
Oxadiazole
Anti-tumor
EGFR

ABSTRACT

A series of 2-(benzylthio)-5-aryloxadiazole derivatives have been designed and synthesized, and their biological activities are also evaluated for EGFR inhibitory activity. Fourteen compounds among the twenty compounds are reported for the first time. Their chemical structures are characterized by ^{1}H NMR, MS, and elemental analysis. Anti-proliferative and EGFR inhibition assay results have demonstrated that compound **3e** shows the most potent biological activity (IC_{50} = 1.09 μM for MCF-7 and IC_{50} = 1.51 μM for EGFR). Docking simulation has been performed to position compound **3e** into the EGFR active site to determine the probable binding model, with an estimated binding free energy value of −10.7 kcal/mol. Compound **3e** with potent inhibitory activity in tumor growth inhibition may be a promising anti-tumor leading compound for the further research.

Crown Copyright © 2011 Published by Elsevier Masson SAS. All rights reserved.

1. Introduction

The epidermal growth factor receptor (EGFR), a transmembrane protein tyrosine kinase (PTK) that is activated by ligand-induced dimerization, plays a critical role in regulating cell proliferation, differentiation, and migration [1]. The up-regulated activity of EGFR correlates with many human tumors, including head and neck, lung, breast, bladder, prostate, and kidney cancers [2–7]. It has been also observed the overexpression of EGFR in breast cancer, ovarian cancer and so on [8]. Therefore, EGFR tyrosine kinase represents an attractive target for the development of novel anti-cancer agents. In the past few years, large numbers of small organic molecules have been employed to inhibit kinase function by targeting the ATP binding site of EGFR tyrosine kinase. Gefitinib (Iressa) and erlotinib (Tarceva) are the representative drugs for this kind of inhibitors and have been approved by US FDA for treatment of patients with non small-cell-lung cancer (NSCLC) [9,10].

Compounds containing an oxazole or oxadiazole ring, which is as a building element can be seen in many natural products, have various activities such as hypoglycemic [11], anti-fungal [12], anti-inflammatory [13], and anti-bacterial activities [14]. In the area of anti-tumor agents, for example, Harris et.al have reported that 2-anilino-5-aryloxazoles can be as a novel class of VEGFR2 (Vascular Endothelial Growth Factor Receptor 2, also called the Kinase insert Domain containing Receptor, KDR) kinase inhibitors. The structure-activity relationships as well as the enzyme binding model are also illustrated. In this model, 2-anilino-5-aryloxazoles bonds to the ATP binding site of KDR kinase. The central oxazole ring comprises the core structure of the compound and interacts with Cys919 of the peptide backbone *via* hydrogen acceptor bonding with the oxazole nitrogen [15].

To our knowledge, 2-thiol-5-aryloxadiazoles as a potential anti-fungal agent attracts much attention. However, there are few reports involving in the anti-tumor activity, especially for EGFR inhibitory activity of 2-(benzylthio)-5-aryloxadiazole derivatives. We have performed a virtual screening of these substituted oxadiazole derivatives by AutoDock Tools, including *ortho*-substitution, *meta*-substitution and *para*-substitution. The results reveal that all compounds would have potent EGFR inhibitory activity, with an estimated binding free energy ranging from about −8 kcal/mol to −13 kcal/mol. The corresponding inhibition constant can come to nM level. Virtual screening results also predict that *ortho*-substitution at the 5-phenyl ring would access active site and might have better EGFR inhibitory activity. As a result, we hope to discover a potential effective compound from these 2-(benzylthio)-5-aryloxadiazole derivatives that can be as the leading compound for the further optimal research.

Herein, in order to extend our research on anticancer compounds with EGFR inhibitory activity, a series of 2-(benzylthio)-5-aryloxadiazole derivatives are synthesized and evaluated with EGFR inhibitory activity. Thirteen compounds(**3d**–**3j**, **3l**–**3n** and **3r**–**3t**) are reported for the first time, **3a**-**3c**, **3k** and

* Corresponding author. Tel./fax: +86 25 8359 2672.
E-mail address: zhuhl@nju.edu.cn (H.-L. Zhu).

0223-5234/$ – see front matter Crown Copyright © 2011 Published by Elsevier Masson SAS. All rights reserved.
doi:10.1016/j.ejmech.2011.11.015

3o–**3q** have been published [16,17]. The structure-activity relationships and possible enzyme binding mode which is predicted by molecular docking research are also illustrated.

2. Results and discussion

2.1. Chemistry

The general synthesis of various substituted 2-(benzylthio)-5-phenyl-1,3,4-oxadiazole derivatives were depicted in Scheme 1, 2. Most substituted benzoylhydrazine were obtained from commercial resource, but a few of them still needed to be prepared using the published methods from corresponding acids or esters in about medium yields [16–19]. It was a reaction of two steps to obtain the key intermediate **1**. Firstly, benzoylhydrazine, carbon disulfide and potassium hydroxide were reacted in 95% ethanol for 24 h, cyclizing to produce potassium salt intermediate. Then the potassium salt intermediate converted to **1** by adjusting the pH value. Finally, the direct condensation between **1** and **2** led to the formation of end product **3a**–**3t** (Table 1) under basic condition in room temperature with a high yield. However, the total yields were moderate due to the low yields of intermediate. All of the synthetic compounds gave satisfactory analytical and spectroscopic data, which were in full accordance with their depicted structures.

2.2. The anti-proliferative activity and structure-activity relationship (SAR) study

All the compounds **3a**–**3t** were evaluated for cytotoxic properties on two human tumor cell lines, breast adeno carcinoma cell line MCF-7 and lung adeno carcinoma cell line A549, one mouse skin melanoma cell line B16-F10 with gefitinib as a standard. The inhibitory effects on cell proliferation were determined by MTT assay [20]. The inhibitory potency (IC_{50}) of compounds **3a**–**3t** were given in Table 2. The IC_{50} values were the average of at least three independent experiments.

As shown in Table 2, it was observed that 5-aryloxadiazole derivatives had been found to show the inhibition of growth of three tumor cell lines with moderate IC_{50} values. For MCF-7 cell line which over-expressed EGFR that previously references had reported [21], 5-aryloxadiazole derivatives in particular displayed more potent anti-proliferative activity than the other two tumor cell lines. The IC_{50} values of most 5-aryloxadiazole derivatives ranged from 1.09 μM to 15.1 μM in MCF-7. Among them, compound **3e** displayed the most potent anti-proliferative activity with IC_{50} of 1.09 μM, comparable to the positive control gefitinib (IC_{50} = 12.05 μM). Nevertheless, IC_{50} values would have a 2–18 folds decrease in A549 and 1–10 folds in B16-F10 on average. More potent anti-proliferative activity for MCF-7 together with virtual screening results both indicated that the over-expressed EGFR might be a potential target which these 5-aryloxadiazole derivatives interacted with.

Structure-activity relationships at cellular level for these 5-aryloxadiazole derivatives demonstrated that compounds with substitution of benzene ring (**3a**–**3p**) showed more potent activities than those with substitution of pyridine ring (**3q**–**3t**). For benzene substituent, substituents at *ortho* position (**3b**–**3g**) might have an increase of activity than those at the *para* position. In particular, compound **3e** exhibited the most potent anti-proliferative activity with IC_{50} value of 1.09 μM. A comparison of *ortho* position substitution on benzene ring indicated that a *ortho* electron donating group had slightly improved anti-proliferative activity. Compared to **3a**, substitution at the *para* position led to

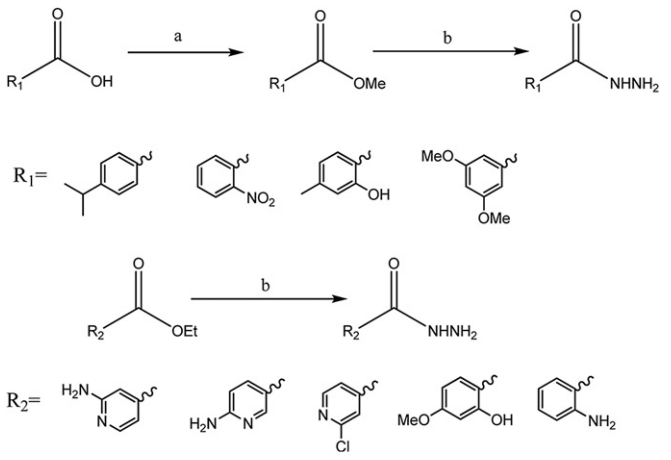

Scheme 1. General synthesis of substituted benzoylhydrazine from corresponding substituted acids and esters. Reagents and conditions: (a) 98% H_2SO_4, methanol, reflux, **6h**; (b) 85% $NH_2NH_2.H_2O$, ethanol, reflux, **3h**.

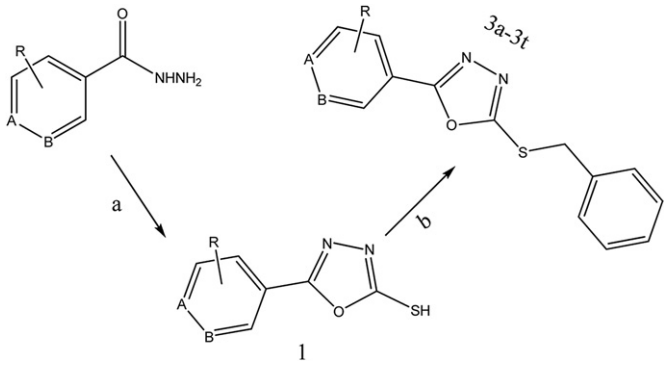

Scheme 2. General synthesis of 2-(benzylthio)-5-aryloxadiazole derivatives **3a**–**3t**. Reagents and conditions: (a) i KOH/CS_2, 95% ethanol, reflux, 24h; ii HCl/pH5-6; (b) Benzyl bromide, NaOH, 80% ethanol, rt, **3h**.

Table 1
Structure of 2-(benzylthio)-5-aryloxadiazole derivatives **3a**–**3t**.

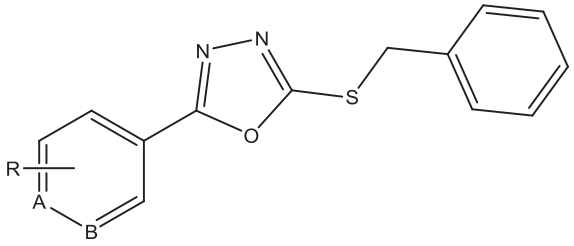

Compd.	R	A	B	Compd.	R	A	B
3a	H	CH	CH	**3k**	4-Cl	CH	CH
3b	2-F	CH	CH	**3l**	2–OH, 4-Me	CH	CH
3c	2–CH_3	CH	CH	**3m**	2–OH, 4-OMe	CH	CH
3d	2–NO_2	CH	CH	**3n**	3,5-di-OMe	CH	CH
3e	2–NH_2	CH	CH	**3o**	4-F	CH	CH
3f	2-OEt	CH	CH	**3p**	4-NMe_2	CH	CH
3g	2-OMe	CH	CH	**3q**	H	N	CH
3h	4-t-Bu	CH	CH	**3r**	2–NH_2	N	CH
3i	4-i-Pr	CH	CH	**3s**	2-Cl	N	CH
3j	4–NH_2	CH	CH	**3t**	2–NH_2	CH	N

Table 2
Anti-proliferative activity in 3 tumor cell lines and EGFR inhibitory activity of top 10 compounds.

Compd.	IC_{50}, μM				Compd.	IC_{50}, μM			
	MCF-7	A549	B16-F10	EGFR		MCF-7	A549	B16-F10	EGFR
Gefitinib	12.05	10.08	–	0.02					
3a	3.89	30.3	24.7	16.63	**3k**	31.7	52.1	21.0	nt
3b	2.11	22.9	23.0	5.11	**3l**	9.12	29.2	9.0	34.25
3c	2.69	31.2	19.9	5.72	**3m**	15.1	27.9	13.7	nt
3d	5.92	47.0	20.3	38.32	**3n**	7.81	20.0	6.8	26.06
3e	1.09	18.2	10.3	1.51	**3o**	13.3	30.7	22.0	nt
3f	5.31	34.0	17.9	38.43	**3p**	39.0	75.5	41.1	nt
3g	8.11	42.7	19.3	12.32	**3q**	38.5	78.5	48.2	nt
3h	3.29	18.6	9.2	7.44	**3r**	30.0	68.7	45.1	nt
3i	15.6	29.7	8.8	nt	**3s**	29.2	65.6	35.1	nt
3j	38.4	76.5	41.3	nt	**3t**	41.8	60.0	44.6	nt

nt, not test.

a significant loss of activity, whether with substitution of electron donating groups (**3h**, **3i**) or electron withdrawing (**3k**, **3o**) groups. In addition, considering the effect of the number of substituents of benzene ring, we designed and evaluated the compounds with two substituents at 2,4-position (**3l**, **3m**) or 3,5-position (**3n**). Nevertheless, there was also no notable improvement compared to the other mono-substituted derivatives.

2.3. EGFR inhibitory activity and molecular docking study

Based on the potent anti-proliferative activity in MCF-7 cell line, furthermore, we had selected the top 10 compounds (**3a**–**3h**, **3l**, **3n**), which had the best anti-proliferative activity results among the 20 compounds for MCF-7, and tested their EGFR inhibitory activity to get an insight whether these compounds acted through EGFR-TKI pathway. As shown in Table 2, all compounds had EGFR inhibitory activity. Compound **3e**, in particular, exhibited the most potent inhibitory activity consistent with anti-proliferative assay results (IC_{50} = 1.51 μM). Then, an analysis between EGFR enzyme inhibition and inhibition of MCF-7 cellular proliferation of the top 10 compounds indicated that there was a moderate correlation between EGFR enzyme inhibition and inhibition of MCF-7 cellular proliferation, as evidenced in Fig. 1, with a correlation coefficient of 0.72, R square value 0.805. However, a discrepancy was also observed between enzyme inhibition and cell anti-proliferation that the anti-proliferative activity of these dioxazole derivatives could be comparable to gefinitib but EGFR inhibitory activity is much less than it. This might suggested that they were acting as multi-kinase inhibitor, EGFR was one of their targets. In general, these compounds could inhibit EGFR enzyme, subsequently inhibited the proliferation of MCF-7.

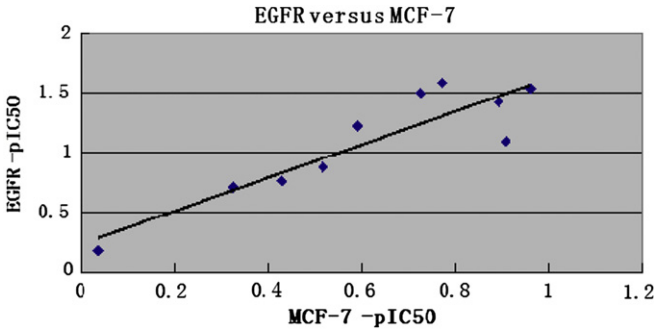

Fig. 1. Correlation between -pIC50's for the inhibition of EGFR enzyme and MCF-7 cellular proliferation, $r = 0.72$, $R^2 = 0.805$.

In order to gain more understanding of the interaction with EGFR, molecular docking of the most potent inhibitor **3e** into ATP binding site of EGFR kinase was performed on a binding model based on the EGFR complex structure (1M17.pdb). The binding model of compound **3e** and EGFR was depicted in Fig. 2.

Previously research had revaled that the binding model of gefitinib was strikingly similar to erlotinib. Both quinazoline ring of gefitinib and erlotinib were oriented with the 1-N in the back of the ATP binding pocket. Interestingly, unlike most kinase inhibitors, both they formed only a single hydrogen bond. Gefitinib's hydrogen bond formed with the mainchain amide of Met 793 while the N1 of the quinazoline of erlotinib accepted an H-bond from the Met769 amide nitrogen [22,23].

Compared to the binding model of gefitinib and erlotinib, compound **3e** was also projected into the ATP binding pocket with a quite smooth conformation, and was nicely bound to the EGFR kinase with its N atom forming a H-bond interaction with Pro770. This H-bond might be favor to the EGFR inhibitory activity. The 2-benzyl group orientated toward the front of the pocket. As the same as the quinazoline ring of erlotinib, the 5-phenyl ring was also in the back of the pocket and was much close to the active residue Met769. Met769 was a critical amino residue in the active site which was previously mentioned for erlotinib. Though direct H-bond interaction with Met769 was not observed in this model, NH_2 group of 5-phenyl ring was such close to this residue that we could believe that the further modification of this group might bring improved EGFR inhibitory activity.

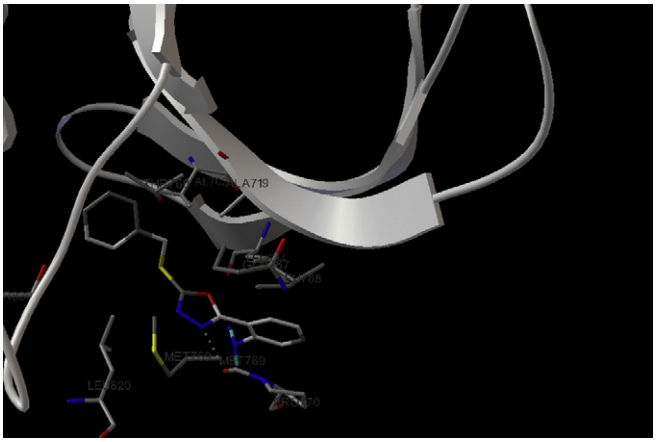

Fig. 2. Molecular docking modeling of compound 3e with EGFR kinase shows intra-molecular hydrogen bonds with Pro770. Note: For clarity, only interacting residues are displayed. The H-bond is displayed as dot line.

3. Conclusions

A series of 2-(benzylthio)-5-aryloxadiazole derivatives have been designed and synthesized, and their biological activities have also been evaluated as potent EGFR inhibitor. Most compounds showed moderate inhibition against MCF-7, A549 and B16-F10 cell lines. Compound **3e** demonstrated the most potent anti-proliferative activity and EGFR inhibitory activity. Docking simulation result shows compound **3e** was stabilized by hydrogen bonding interactions. In general, our current findings regarding EGFR tyrosine kinase inhibition of compounds containing (benzylthio)oxadiazole framework are completely new. This study further presents (benzylthio)oxadiazole framework as new class of anti-tumor agents and it may serve as model compounds for design and development of therapeutic based anticancer agents.

4. Experimental section

4.1. General

All commercially available reagents were obtained from various producers and used without further purification. The reactions were monitored and the purity of the compounds was checked by thin layer chromatography (TLC) using aluminum sheets with Silica Gel 60 F_{254} (Merck). Melting points (uncorrected) were determined on a XT4MP apparatus (Taike Corp., Beijing, China). ESI mass spectra were obtained on a Mariner System 5304 mass spectrometer, and ^{1}H NMR spectra were recorded on a Bruker DPX300 spectrometer at 25 °C with TMS and solvent signals allotted as internal standards. Chemical shifts were reported in ppm (δ). Elemental analyses were performed on a CHN-O-Rapid instrument and were within ±0.4% of the theoretical values.

4.2. General procedure for the synthesis of 5-phenyl-1,3,4-oxadiazole-2-thiol derivatives

For the synthesis of substituted benzoylhydrazines, a mixture of corresponding esters (20 mmol), 85% hydrazine hydrate (20 mmol) in ethanol (35 ml) was heated to reflux for 5 h. After that, the solution was poured into ice-water. The precipitate was filtered and crystallized from ethanol.

Then equimolar portions of the appropriately substituted benzoylhydrazine (5 mmol) and potassium hydroxide (5 mmol) were dissolved in 20 mL of 95% ethanol. The mixture was allowed to stir for several minutes at room temperature and then carbon disulfide (7.5 mmol) was slowly added dropwise to the reaction system *via* a self-equalizing addition funnel while the mixture was heated to reflux. After 24 h, the solvent was completely removed under reduced pressure. The residue obtained was dissolved in water (50 mL) and diluted hydrochloric acid was added to adjust the pH values of the solution to 5–6. Then the precipitate was collected by filtering under reduced pressure, washed with water for several times and dried without further purification.

4.3. General procedure for the synthesis of 2-(benzylthio)-5-phenyl-1,3,4-oxadiazole derivatives (**3a**–**3t**)

The synthesis of all compounds adopted the following procedure: to a solution of substituted 5-phenyl-1,3,4-oxadiazole-2-thiol (1 mmol) in 80% ethanol benzyl bromide (1.1 mmol) was added slowly and stirred at room temperature for 10 min, then 5 mL (8%, w/w) sodium hydroxide solution was added dropwise to the reaction mixture, stirred for another 3 h [16]. Most commonly, a precipitate was formed when the solution was poured into ice-water, filtered and recrystallized from ethanol, washed with cool ethanol for three times.

4.3.1. 2-(Benzylthio)-5-phenyl-1,3,4-oxadiazole (**3a**)

White powder. Yield, 95%. Mp 94–95 °C. ^{1}H NMR (300 MHz, $CDCl_3$): δ 4.53 (*s*, 2H, CH_2), 7.30–7.38 (*m*, 3H), 7.45–7.53 (*m*, 5H), 7.97–8.00 (*m*, 2H). MS (ESI): 268.1 ($C_{15}H_{12}N_2OS$ $[M + H]^+$). Anal. Calcd for $C_{15}H_{11}N_2OS$: C, 67.14; H, 4.51; N, 10.44. Found: C, 67.36; H, 4.63; N, 10.73%.

4.3.2. 2-(Benzylthio)-5-(2-fluorophenyl)-1,3,4-oxadiazole (**3b**)

White crystal. Yield, 55%. Mp 61–62 °C. ^{1}H NMR (300 MHz, $CDCl_3$): δ 4.54 (*s*, 2H, CH_2), 7.22 (*d*, *J* = 8.5 Hz, 1H), 7.28–7.36 (*m*, 4H), 7.46 (*d*, *J* = 7.2 Hz, 2H), 7.50–7.54 (*m*, 1H), 7.98–8.01 (*m*, 1H). MS (ESI): 286.1 ($C_{15}H_{11}FN_2OS$ $[M + H]^+$). Anal. Calcd for $C_{15}H_{10}FN_2OS$: C, 62.92; H, 3.87; N, 9.78. Found: C, 63.06; H, 4.03; N, 9.53%.

4.3.3. 2-(Benzylthio)-5-o-tolyl-1,3,4-oxadiazole (**3c**)

White powder. Yield, 70%. Mp 105–106 °C. ^{1}H NMR (300 MHz, $CDCl_3$): δ 2.68 (*s*, 3H), 4.53 (*s*, 2H, CH_2), 7.30–7.40 (*m*, 6H), 7.47 (*d*, *J* = 6.2 Hz, 2H), 7.84 (*d*, *J* = 6.75 Hz, 1H). MS (ESI): 282.1 ($C_{16}H_{14}N_2OS$ $[M + H]^+$). Anal. Calcd for $C_{16}H_{13}N_2OS$: C, 68.06; H, 5.00; N, 9.92. Found: C, 67.86; H, 5.13; N, 9.73%.

4.3.4. 2-(Benzylthio)-5-(2-nitrophenyl)-1,3,4-oxadiazole (**3d**)

Yellow crystal. Yield, 90%. Mp 120–121 °C. ^{1}H NMR (300 MHz, $CDCl_3$): δ 4.52 (*s*, 2H, CH_2), 7.30–7.38 (*m*, 3H), 7.45 (*d*, *J* = 7.68 Hz, 2H), 7.70–7.78 (*m*, 2H), 7.92–7.95 (*m*, 1H), 8.01–8.04 (*m*, 1H). MS (ESI): 313.1 ($C_{15}H_{11}N_3O_3S$ $[M + H]^+$). Anal. Calcd for $C_{15}H_{10}N_3O_3S$: C, 57.50; H, 3.54; N, 13.41. Found: C, 57.66; H, 3.68; N, 13.63%.

4.3.5. 2-(5-(benzylthio)-1,3,4-oxadiazol-2-yl)aniline (**3e**)

White powder. Yield, 95%. Mp 86–87 °C. ^{1}H NMR (300 MHz, $CDCl_3$): δ 4.52 (*s*, 2H, CH_2), 5.77(brs, 2H), 6.71–6.79(*m*, 2H), 7.29–7.39 (*m*, 4H), 7.46(*d*, *J* = 7.5 Hz, 2H), 7.65(*d*, *J* = 7.86 Hz, 1H). MS (ESI): 283.1 ($C_{15}H_{13}N_3OS$ $[M + H]^+$). Anal. Calcd for $C_{15}H_{12}N_3OS$: C, 63.58; H, 4.62; N, 14.83. Found: C, 63.71; H, 4.68; N, 14.63%.

4.3.6. 2-(Benzylthio)-5-(2-ethoxyphenyl)-1,3,4-oxadiazole (**3f**)

Light yellow powder. Yield, 93%. Mp 69–70 °C. ^{1}H NMR (300 MHz, $CDCl_3$): δ 1.47 (*t*, *J* = 6.94 Hz, 3H), 4.13–4.20 (*q*, *J* = 6.93 Hz, 2H), 4.52 (*s*, 2H, CH_2), 7.03 (*t*, *J* = 8.05 Hz, 2H), 7.29–7.37 (*m*, 3H), 7.43–7.49 (*m*, 3H), 7.86–7.89 (*m*, 1H). MS (ESI): 312.1 ($C_{17}H_{16}N_2O_2S$ $[M + H]^+$). Anal. Calcd for $C_{17}H_{15}N_2O_2S$: C, 65.36; H, 5.16; N, 8.97. Found: C, 65.21; H, 5.28; N, 8.78%.

4.3.7. 2-(Benzylthio)-5-(2-methoxyphenyl)-1,3,4-oxadiazole (**3g**)

White powder. Yield, 80%. Mp 48–50 °C. ^{1}H NMR (300 MHz, $CDCl_3$): δ 3.95 (*s*, 3H), 4.52(*s*, 2H, CH_2), 7.06 (*t*, *J* = 7.41 Hz, 2H), 7.29–7.37 (*m*, 3H), 7.46–7.52 (*m*, 3H), 7.84–7.87 (*m*, 1H). MS (ESI): 298.1 ($C_{16}H_{14}N_2O_2S$ $[M + H]^+$). Anal. Calcd for $C_{16}H_{13}N_2O_2S$: C, 64.41; H, 4.73; N, 9.39. Found: C, 64.23; H, 4.84; N, 9.58%.

4.3.8. 2-(Benzylthio)-5-(4-tert-butylphenyl)-1,3,4-oxadiazole (**3h**)

White powder. Yield, 52%. Mp 66–67 °C. ^{1}H NMR (300 MHz, $CDCl_3$): δ 1.35 (*s*, 9H), 4.52 (*s*, 2H, CH_2), 7.29–7.37 (*m*, 3H), 7.44–7.47 (*m*, 2H), 7.50 (*d*, *J* = 8.4 Hz, 2H), 7.91 (*d*, *J* = 8.43 Hz, 2H). MS (ESI): 324.1 ($C_{19}H_{20}N_2OS$, $[M + H]^+$). Anal. Calcd for $C_{19}H_{19}N_2OS$: C, 70.34; H, 6.21; N, 8.63. Found: C, 70.48; H, 6.35; N, 8.51%.

4.3.9. 2-(Benzylthio)-5-(4-isopropylphenyl)-1,3,4-oxadiazole (**3i**)

Yellow powder. Yield, 53%. Mp 49–50 °C. ^{1}H NMR (300 MHz, $CDCl_3$): δ 1.28 (*d*, *J* = 6.93 Hz, 6H), 2.94–2.99 (*m*, 1H), 4.52 (*s*, 2H, CH_2), 7.29–7.35 (*m*, 5H), 7.45 (*d*, *J* = 7.68 Hz, 2H), 7.91 (*d*, *J* = 8.25 Hz, 2H). MS (ESI): 310.1 ($C_{18}H_{18}N_2OS$ $[M + H]^+$). Anal. Calcd for

$C_{18}H_{17}N_2OS$: C, 69.65; H, 5.84; N, 9.02. Found: C, 69.78; H, 5.95; N, 8.89%.

*4.3.10. 4-(5-(Benzylthio)-1,3,4-oxadiazol-2-yl)aniline (**3j**)*

Yellow powder. Yield, 85%. Mp 123–124 °C. ^{1}H NMR (300 MHz, $CDCl_3$): δ 4.49 (*s*, 2H, CH_2), 6.71 (*d*, J = 8.79 Hz, 2H), 7.28–7.37 (*m*, 3H), 7.45 (*d*, J = 6.39 Hz, 2H), 7.78 (*d*, J = 6.75 Hz, 2H). MS (ESI): 283.1 ($C_{15}H_{13}N_3OS$ [M + H]$^+$). Anal. Calcd for $C_{15}H_{12}N_3OS$: C, 63.58; H, 4.62; N, 14.83. Found: C, 63.78; H, 4.75; N, 14.99%.

*4.3.11. 2-(Benzylthio)-5-(4-chlorophenyl)-1,3,4-oxadiazole (**3k**)*

White powder. Yield, 78%. Mp 119–120 °C. ^{1}H NMR (300 MHz, $CDCl_3$): δ 4.53 (*s*, 2H, CH_2), 7.30–7.38 (*m*, 3H), 7.45–7.49 (*m*, 4H), 7.91–7.94 (*m*, 2H). MS (ESI): 302.1 ($C_{15}H_{11}ClN_2OS$ [M + H]$^+$). Anal. Calcd for $C_{15}H_{10}ClN_2OS$: C, 59.50; H, 3.66; N, 9.25. Found: C, 59.65; H, 3.75; N, 9.09%.

*4.3.12. 2-(5-(Benzylthio)-1,3,4-oxadiazol-2-yl)-5-methylphenol (**3l**)*

White powder. Yield, 97%. Mp 93–94 °C. ^{1}H NMR (300 MHz, $CDCl_3$): δ 2.37 (*s*, 3H), 4.52 (*s*, 2H, CH_2), 6.80 (*d*, J = 8.04 Hz, 1H), 6.92 (*s*, 1H), 7.30–7.39 (*m*, 3H), 7.46 (*d*, J = 6.39 Hz, 2H), 7.55 (*d*, J = 8.04 Hz, 1H), 9.80 (*s*, 1H). MS (ESI): 298.1 ($C_{16}H_{14}N_2O_2S$, [M + H]$^+$). Anal. Calcd for $C_{16}H_{13}N_2O_2S$: C, 64.41; H, 4.73; N, 9.39. Found: C, 64.58; H, 4.85; N, 9.19%.

*4.3.13. 2-(5-(Benzylthio)-1,3,4-oxadiazol-2-yl)-5-methoxyphenol (**3m**)*

Colorless crystal. Yield, 91%. Mp 139–140 °C. ^{1}H NMR (300 MHz, $CDCl_3$): δ 3.84 (*s*, 3H), 4.51 (*s*, 2H, CH_2), 6.53–6.57 (*m*, 1H), 6.60 (*s*, 1H), 7.31–7.36 (*m*, 3H), 7.44–7.47 (*m*, 2H), 7.56 (*d*, J = 8.79 Hz, 1H), 10.00 (*s*, 1H). MS (ESI): 314.1 ($C_{16}H_{14}N_2O_3S$ [M + H]$^+$). Anal. Calcd for $C_{16}H_{13}N_2O_3S$: C, 61.13; H, 4.49; N, 8.91. Found: C, 61.38; H, 4.35; N, 9.09%.

*4.3.14. 2-(Benzylthio)-5-(3,5-dimethoxyphenyl)-1,3,4-oxadiazole (**3n**)*

White powder. Yield, 93%. Mp 109–110 °C. ^{1}H NMR (300 MHz, $CDCl_3$): δ 3.85 (*s*, 6H), 4.52 (*s*, 2H, CH_2), 6.60 (*t*, J = 2.38 Hz, 1H), 7.13 (*d*, J = 2.19 Hz, 2H), 7.30–7.38 (*m*, 3H), 7.45–7.47 (*m*, 2H). MS (ESI): 328.1 ($C_{17}H_{16}N_2O_3S$ [M + H]$^+$). Anal. Calcd for $C_{17}H_{15}N_2O_3S$: C, 62.18; H, 4.91; N, 8.53. Found: C, 62.35; H, 4.75; N, 8.69%.

*4.3.15. 2-(Benzylthio)-5-(4-fluorophenyl)-1,3,4-oxadiazole (**3o**)*

Colorless crystal. Yield, 60%. Mp 96–97 °C. ^{1}H NMR (300 MHz, $CDCl_3$): δ 4.53 (*s*, 2H, CH_2), 7.18 (*t*, J = 8.6 Hz, 2H), 7.30–7.38 (*m*, 3H), 7.44–7.47 (*m*, 2H), 7.97–8.01 (*m*, 2H). MS (ESI): 286.1 ($C_{15}H_{11}FN_2OS$ [M + H]$^+$). Anal. Calcd for $C_{15}H_{10}FN_2OS$: C, 62.92; H, 3.87; N, 9.78. Found: C, 62.72; H, 4.01; N, 9.59%.

*4.3.16. 4-(5-(Benzylthio)-1,3,4-oxadiazol-2-yl)-N,N-dimethylaniline (**3p**)*

Yellow crystal. Yield, 88%. Mp 158–159 °C. ^{1}H NMR (300 MHz, $CDCl_3$): δ 3.06 (*s*, 6H), 4.53 (*s*, 2H, CH_2), 6.56 (*d*, J = 8.79 Hz, 1H), 6.79 (*s*, 2H), 7.29–7.36 (*m*, 3H), 7.45 (*d*, J = 6.78 Hz, 2H), 7.83–7.86 (*m*, 1H). MS (ESI): 311.1 ($C_{17}H_{17}N_3OS$ [M + H]$^+$). Anal. Calcd for $C_{17}H_{16}N_3OS$: C, 65.57; H, 5.50; N, 13.49. Found: C, 65.72; H, 4.91; N, 13.69%.

*4.3.17. 2-(Benzylthio)-5-(pyridin-4-yl)-1,3,4-oxadiazole (**3q**)*

Dark green crystal. Yield, 65%. Mp 103–104 °C. ^{1}H NMR (300 MHz, $CDCl_3$): δ 4.56 (*s*, 2H, CH_2), 7.31–7.39 (*m*, 3H), 7.45–7.48 (*m*, 2H), 7.83–7.85 (*m*, 2H). MS (ESI): 269.1 ($C_{14}H_{11}N_3OS$ [M + H]$^+$). Anal. Calcd for $C_{14}H_{10}N_3OS$: C, 62.43; H, 4.12; N, 15.60. Found: C, 62.25; H, 4.25; N, 15.79%.

*4.3.18. 4-(5-(Benzylthio)-1,3,4-oxadiazol-2-yl)pyridin-2-amine (**3r**)*

Light yellow powder. Yield, 72%. Mp 187–188 °C. ^{1}H NMR (300 MHz, $CDCl_3$): δ 4.54 (*s*, 2H, CH_2), 4.66 (*s*, 2H), 7.05 (*s*, 1H), 7.17–7.19 (*m*, 1H), 7.30–7.38 (*m*, 3H), 7.44–7.47 (*m*, 2H), 8.21 (*d*, J = 5.31 Hz, 1H). MS (ESI): 284.1 ($C_{14}H_{12}N_4OS$ [M + H]$^+$). Anal. Calcd for $C_{14}H_{11}N_4OS$: C, 59.14; H, 4.25; N, 19.70. Found: C, 59.35; H, 4.35; N, 19.49%.

*4.3.19. 2-(Benzylthio)-5-(2-chloropyridin-4-yl)-1,3,4-oxadiazole (**3s**)*

White powder. Yield, 98%. Mp 80–81 °C. ^{1}H NMR (300 MHz, $CDCl_3$): δ 4.56 (*s*, 2H, CH_2), 7.32–7.39 (*m*, 3H), 7.45–7.48 (*m*, 2H), 7.77–7.79 (*m*, 1H), 7.87 (*s*, 1H), 8.56 (*d*, J = 5.1 Hz, 1H). MS (ESI): 303.1 ($C_{14}H_{10}ClN_3OS$ [M + H]$^+$). Anal. Calcd for $C_{14}H_9ClN_3OS$: C, 55.35; H, 3.32; N, 13.83. Found: C, 59.48; H, 3.45; N, 13.59%.

*4.3.20. 5-(5-(Benzylthio)-1,3,4-oxadiazol-2-yl)pyridin-2-amine (**3t**)*

Yellow powder. Yield, 76%. Mp 156–158 °C. ^{1}H NMR (300 MHz, $CDCl_3$): δ 4.50 (*s*, 2H, CH_2), 4.83 (*s*, 2H), 6.55 (*d*, J = 8.79 Hz, 1H), 7.27–7.39 (*m*, 3H), 7.44 (*d*, J = 7.68 Hz, 2H), 7.98–8.02 (*m*, 1H), 8.65 (*s*, 1H). MS (ESI): 284.1 ($C_{14}H_{12}N_4OS$ [M + H]$^+$). Anal. Calcd for $C_{14}H_{11}N_4OS$: C, 59.14; H, 4.25; N, 19.70. Found: C, 59.27; H, 4.38; N, 19.55%.

4.4. Anti-proliferative assay

The anti-proliferative activities of compounds **3a**–**3t** were determined using a standard (MTT)-based colorimetric assay (Sigma). Briefly, cell lines were seeded at a density of 7×10^3 cells/well 96-well microtiter plates (Costar). After 24 h, exponentially growing cells were exposed to the indicated compounds at final concentrations ranging from 0.1 to 100 μg/mL. After 48 h, cell survival was determined by the addition of an MTT solution (10 μL of 5 mg/mL MTT in PBS). After 4 h, 100 μL of 10% SDS in 0.01 N HCl was added, and the plates were incubated at 37 °C for a further 18 h; optical absorbance was measured at 570 nm on an LX300 Epson Diagnostic microplate reader. Survival ratios are expressed in percentages with respect to untreated cells. IC values were determined from replicates of six wells from at least two independent experiments.

4.5. EGFR inhibitory assay

A 1.6 kb cDNA encoded for the EGFR cytoplasmic domain (EGFR-CD, amino acids 645–1186) were cloned into baculoviral expression vector pFASTBacHTc. A sequence that encodes $(His)_6$ was located at the 50 upstream to the EGFR sequence. Sf-9cells were infected for 3 days for protein expression. Sf-9 cell pellets were solubilized at 0 °C in a buffer at pH 7.4 containing 50 mM HEPES, 10 mM NaCl, 1% Triton, 10 μM ammonium molybdate 100 μM sodium vanadate, 10 μg/mL aprotinin, 10 μg/mL leupeptin, 10 μg/mL pepstatin, and 16 μg/mL benzamidine HCl for 20 min followed by 20 min centrifugation. Crude extract supernatant was passed through an equilibrated Ni-NTA superflow packed column and washed with 10 mM and then100 mM imidazole to remove nonspecifically bound material. Histidine tagged proteins were eluted with 250 and 500 mM imidazole and dialyzed against 50 mM NaCl, 20 mM HEPES, 10% glycerol, and 1 μg/mL each of aprotinin, leupeptin, and pepstatin for 2 h. The entire purification procedure was performed at 4 °C or on ice.

The EGFR kinase assay was set up to assess the level of autophosphorylation based on DELFIA/Time-Resolved Fluorometry. Compounds **3a**–**3g**, **3l**, **3n** were dissolved in 100% DMSO and

diluted to the appropriate concentrations with 25 mM HEPES at pH 7.4. In each well, 10 μL of compound was incubated with 10 μL (5 ng for EGFR) of recombinant enzyme (1:80 dilution in 100 mM HEPES) for 10 min at room temperature. Then, 10 μL of 5 mM buffer (containing 20 mM HEPES, 2 mM $MnCl_2$, 100 μM Na_3VO_4, and 1 mM DTT) and 20 μL of 0.1 mM ATP-50 mM $MgCl_2$ was added for 1 h. Positive and negative controls were included in each plate by incubation of enzyme with or without ATP-$MgCl_2$. At the end of incubation, liquid was aspirated, and plates were washed three times with wash buffer. A 75 μL (400 ng) sample of europiumlabeled anti-phosphotyrosine antibody was added to each well for another 1 h of incubation. After washing, enhancement solution was added and the signal was detected by Victor (Wallac Inc) with excitation at 340 nm and emission at 615 nm. The percentage of autophosphorylation inhibition by the compounds was calculated using the following equation: 100%-[(negative control)/(positive control-negative control)]. The IC_{50} was obtained from curves of percentage inhibition with eight concentrations of compound. As the contaminants in the enzyme preparation are fairly low, the majority of the signal was detected by the anti-phosphorylation antibody is from EGFR.

4.6. Molecular docking study

The automated docking studies were carried out using AutoDock version 4.0. First, AutoGrid component of the program pre-calculates a three-dimensional grid of interaction energies based on the macromolecular target using the AMBER force field. The cubic grid box of 60 Å size (x, y, z) with a spacing of 0.375 Å and grid maps were created representing 17 the catalytic active target site region where the native ligand was embedded. Then automated docking studies were carried out to evaluate the binding free energy of the inhibitors within the macromolecules.

The three-dimensional structures of the aforementioned compounds were constructed using Chem3D ultra 11.0 software [Chemical Structure Drawing Standard; Cambridge Soft corporation, USA (2009)], then they were energetically minimized by using MOPAC with 100 iterations and minimum RMS gradient of 0.10. The Gasteiger-Hückel charges of ligands were assigned. The crystal structures of EGFR (PDB code: 1M17) complex were retrieved from the RCSB Protein Data Bank. All bound waters and ligands were eliminated from the protein and the polar hydrogens and the kollman-united charges were added to the protein.

Acknowledgments

This work was supported by Jiangsu National Science Foundation (No. BK2009239).

References

[1] X.W. Zhang, J. Gureasko, K. Shen, P.A. Cole, J. Kuriyan, Cell 125 (2006) 1137–1149.
[2] P.B. Jensen, T. Hunter, Nature 411 (2001) 355–365.
[3] H. Kim, W.J. Muller, Exp. Cell Res. 253 (1999) 78–87.
[4] J. Albanell, J.C. Servat, F. Rojo, J.M. Del Campo, S. Sauleda, J. Anido, G. Raspall, J. Giralt, J. Rosello, R.I. Nicholson, J. Mendelsohn, J. Baselga, Cancer Res. 61 (2001) 6500–6510.
[5] G. Cox, M. Vyberg, B. Melgaard, J. Askaa, A. Oster, K. O'Byrne, Int. J. Cancer 92 (2001) 480–483.
[6] W.J. Gullick, Br. Med. Bull. 47 (1991) 87–98.
[7] D.K. Moscatello, M. Holgado-Mudruga, A.K. Godwin, G. Ramirez, G. Gunn, P.W. Zoltick, J.A. Biegel, R.L. Hayes, A.J. Wong, Cancer Res. 55 (1995) 5536–5539.
[8] D. Scheurle, M. Jahanzeb, R.S. Aronsohn, L. Watzek, R.H. Narayanan, Anticancer. Res. 20 (2000) 2091–2096.
[9] J. Anido, P. Matar, J. Albanell, M. Guzman, F. Rojo, J. Arribas, S. Averbuch, J. Baselga, Clin. Cancer Res. 9 (2003) 1274–1283.
[10] V. Chandregowda, G.V. Rao, G.C. Reddy, Org. Process Res. Dev. 11 (2007) 813–816.
[11] P. Conti, C. Dallanoce, M.D. Amici, C.D. Micheli, K.N. Klotz, Bioorg. Med. Chem. 6 (1998) 401–409.
[12] A. Mishra, S.K. Jain, J.G. Asthana, Orient.J. Chem. 14 (1998) 151–152.
[13] D.H. Ko, M.F. Maponya, M.A. Khalil, E.T. Oriaku, Z. You, J. Med. Chem. Res. 8 (1998) 313–318.
[14] Y.Y. Kang, K.J. Shin, K.H. Yoo, K.J. Seo, C.Y. Hong, C.S. Lee, S.Y. Park, D.J. Kim, S.W. Park, Bioorg. Med. Chem. Lett. 10 (2000) 95–99.
[15] P.A. Harris, M. Cheung, R.N. Hunter III, M.L. Brown, J.M. Veal, R.T. Nolte, L.P. Wang, W. Liu, R.M. Crosby, J.H. Johnson, A.H. Epperly, R. Kumar, D.K. Luttrell, J.A. Stafford, J. Med. Chem. 48 (2005) 1610–1619.
[16] A. Zarghi, M. Faizi, B. Shafaghi, A. Ahadian, H.R. Khojastehpoor, V. Zanganeh, S.A. Tabatabai, A. Shafiee, Bioorg. Med. Chem. Lett. 15 (2005) 3126–3129.
[17] X. Yan, Z.M. Ge, T.M. Cheng, R.T. Li, J. Chin. Pharm. Sci. 17 (2008) 277–280.
[18] Z.X. Liu, J.L. Zhao, X. Huang, Bioorg. Med. Chem. Lett. 16 (2006) 1828–1830.
[19] F. Macaev, G. Rusu, S. Pogrebnoi, A. Gudima, E. Stingaci, L. Vlad, N. Shvets, F. Kandemirli, A. Dimoglo, R. Reynolds, Bioorg. Med. Chem. 13 (2005) 4842–4850.
[20] Y. Qian, H.J. Zhang, H. Zhang, C. Xu, J. Zhao, H.L. Zhu, Bioorg. Med. Chem. 18 (2010) 4991–4996.
[21] P.C. Lv, H.Q. Li, J. Sun, Y. Zhou, H.L. Zhu, Bioorg. Med. Chem. 18 (2010) 4606–4614.
[22] C.H. Yun, T.J. Boggon, Y.Q. Li, M.S. Woo, H. Greulich, M. Meyerson, M.J. Eck, Cancer Cell. 11 (2007) 217–227.
[23] J. Stamos, M.X. Sliwkowski, C. Eigenbro, J. Bio. Chem. 48 (2002) 46265–46272.